

Technical Notes

TECHNICAL NOTES are short manuscripts describing new developments or important results of a preliminary nature. These Notes cannot exceed 6 manuscript pages and 3 figures; a page of text may be substituted for a figure and vice versa. After informal review by the editors, they may be published within a few months of the date of receipt. Style requirements are the same as for regular contributions (see inside back cover).

Noise Transmission of Skin-Stringer Panels Using a Decaying Wave Method

Donald E. Huntington* and Constantinos S. Lyrintzis†
 San Diego State University, San Diego, California 92182

Introduction

AIRCRAFT skin-stringer-frame fuselages are subjected to many different loading conditions during their operation. This loading produces structural vibration, which results in interior acoustic noise. Although researchers have used analytic formulations to study structure-borne noise transmission into an enclosure,¹⁻⁴ numerical methods are easier to use for a complex problem. This work will examine noise transmission into a rectangular acoustic enclosure from a flexible skin-stringer-frame structure imbedded in one wall, such as in Fig. 1. The solutions to the acoustic equations inside this enclosure are determined, once the motion of the flexible structure is known. Thus, the first task of the solution procedure is the vibration analysis of the skin-stringer-frame structure.

This work will use a finite element-decaying wave method (FEDW) to examine the vibration of the skin-stringer-frame structure imbedded in the acoustic enclosure's wall. The FEDW method combines a finite element technique, transfer-matrix formulation, and wave-propagation approach, retaining the advantages of all these methods: flexibility, ease of formulation, good speed, low memory requirements, accuracy, and numerical stability.⁵ The FEDW method requires that the structure to be analyzed must be damped, effectively one-dimensional, and periodic or piecewise-periodic; the fuselage skin section to be analyzed meets these criteria.

This work will examine noise transmission into a rigid rectangular acoustic enclosure (Fig. 1) from a vibrating fuselage skin structure imbedded in the enclosure's wall. Noise transmission from a three-bay, single-row structure into an enclosure with normal and infinite acoustic impedance in the $z = 0$ and $z = d$ walls will be examined first, and results will be compared to those found in Ref. 1 for these cases. Then, this work will examine noise transmission from a forty-bay structure of one and two rows into an acoustic enclosure, to illustrate the effect of multiple rows upon the interior noise for identical external loading. Wall vibration in each case will be analyzed by the finite element-decaying wave method, as mentioned above.

Problem Formulation

There are two distinct steps in the analysis of noise transmission from a flexible wall into a rectangular acoustic enclosure: the vibration analysis of the flexible wall, and the solution of the acoustic equations inside the enclosure using the wall displacement as a boundary condition. To examine the wall vibration, the

finite element-decaying wave (FEDW) method is used. This method, which is best used for station-to-station vibration response, uses finite element-transfer matrices, as formulated by McDaniel and Eversole,⁶ in wave-propagation techniques used by Yong and Lin.⁷ For further details, see Ref. 5. However, when examining noise transmission, one needs to find the amplitude of vibration at every structural node, to ensure good acoustic results. Since the decaying wave method only computes the output at one station, it is necessary to reformulate a part of the solution for each station, which slows the technique down considerably. Thus, a standard finite element formulation would be rather faster than the FEDW method at finding these amplitudes, although it would use more memory and may not be as accurate.

The next step is to get the solutions of the acoustic equation inside the rectangular acoustic enclosure shown in Fig. 1. The flexible skin-stringer-frame structure is embedded in the $z = d$ surface; all other surfaces are structurally rigid. In addition, the walls at $z = 0$, $x = l$, $y = 0$, and $y = w$ are assumed to be acoustically rigid. The general boundary condition for the acoustic equations at any wall is

$$\frac{\partial p}{\partial n} = -\frac{\rho}{Z_a} \dot{w} - \rho \ddot{w} \quad (1)$$

where $\partial p / \partial n$ is the outward normal derivative of the perturbation pressure p , w is the normal deflection of the wall, ρ is the fluid density, and Z_a is the acoustic impedance of the wall. Structurally rigid walls have $\dot{w} = 0$, while acoustically rigid walls have $Z_a = \infty$; otherwise, Z_a is obtained from available empirical expressions for point impedance.¹⁻⁴

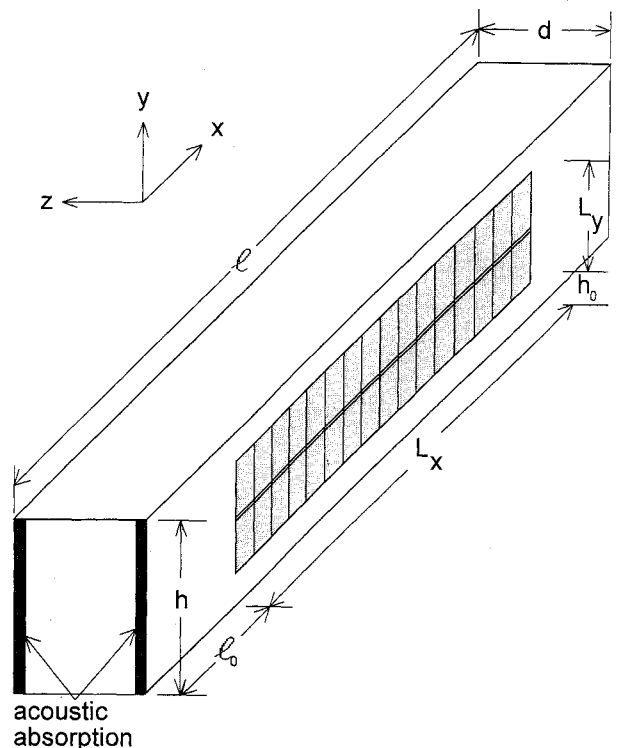


Fig. 1 Geometry of a rectangular acoustic enclosure with a panel-stringer-frame flexible wall.

Received Oct. 3, 1992; revision received March 1, 1993; accepted for publication March 2, 1993. Copyright © 1993 by the American Institute of Aeronautics and Astronautics, Inc. All rights reserved.

*Graduate Research Assistant, Department of Aerospace Engineering and Engineering Mechanics. Member AIAA.

†Associate Professor, Department of Aerospace Engineering and Engineering Mechanics. Member AIAA, ASME.

The solution to the acoustic problem can be found by taking a Fourier transform of the acoustic equation and boundary conditions, and writing the transformed pressure in terms of acoustic hard-wall modes in x and y , with modal coefficients $P_{ij}(z, \omega)$ which involve modal-weighted integrals of wall deflection over the entire flexible surface.^{2,3} Once the P_{ij} are found, one can obtain the sound pressure level (SPL) in decibels at any point in the enclosure:

$$SPL = 10 \log \left\{ S_p \frac{\Delta \omega}{P_0^2} \right\} \quad (2)$$

where S_p is the spectral density of the pressure p , $\Delta \omega$ is a frequency bandwidth, and P_0 is a reference pressure. For more details on the acoustic formulation, see Refs. 1-4.

Numerical Results and Conclusions

This work will use the finite element-decaying wave method and the acoustic procedures mentioned above to examine structure-borne noise transmission into the acoustic enclosure shown in Fig. 1. First, a one-row, three-bay simply supported skin-stringer structure is used for the enclosure's flexible wall; noise transmission results will be compared with those previously published for this case.² Then, the enclosure's flexible wall will have 40 bays and one or two rows, and noise transmission will be examined to illustrate the difference between noise transmission from single-row structures and multiple row structures.

For the vibration analysis of the flexible wall, all material and geometric constants are those of a passenger airliner,⁵ and a structural damping factor of 0.01 is used. Also, the structure is discretized into 4×16 elements per row-bay. For each case, a point load is applied on a stringer midrow, at roughly one-third the flexible wall's length; the load has a truncated Gauss white noise spectral density of $0.003359 \text{ lb}^2/\text{Hz}$ between 10 and 750 Hz, and a spectral density of zero outside that range. For purposes of computing impedance, the acoustic resistivity of the lining is $R = 4 \times 10^4 \text{ mks rayls/m}$, and damping of the fundamental acoustic mode is assumed to be $\zeta_0 = 0.03$. The enclosure's air density and sound speed are $\rho = 1.147 \times 10^{-7} \text{ lb s}^2/\text{in.}^4$, and $c = 13,540 \text{ in./s}$, respectively. Finally, all computations use a frequency spacing $\Delta f = 5 \text{ Hz}$.

An acoustic enclosure with a one-row, three-bay flexible wall was analyzed first. The enclosure had $l = 142 \text{ in.}$, $h = 50 \text{ in.}$, $d = 48 \text{ in.}$, $l_0 = 60 \text{ in.}$, $h_0 = 15 \text{ in.}$, $L_x = 24.6 \text{ in.}$, and $L_y = 20 \text{ in.}$; all lengths are defined in Fig. 1. Figure 2 illustrates the computed SPL at the geometric center of the enclosure for normal and infinite acoustic impedance at the $z = 0$ and $z = d$ walls. These results compare favorably with those published for the same enclosure in Ref. 2, particularly at higher frequency; while the peak amplitudes vary somewhat due to differences in load application, the peaks

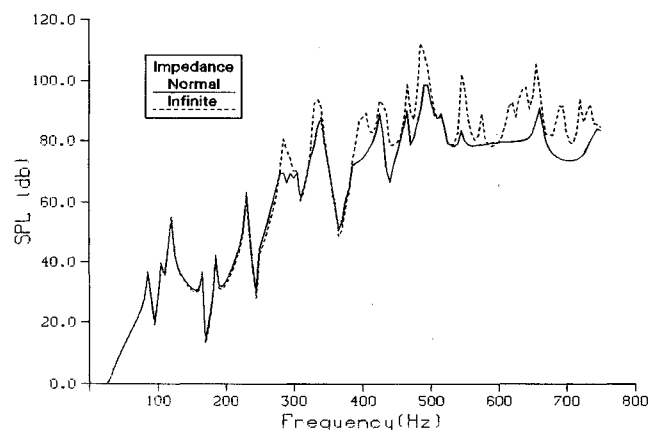


Fig. 2 Sound pressure levels at the center of the three-bay enclosure for different absorption characteristics.

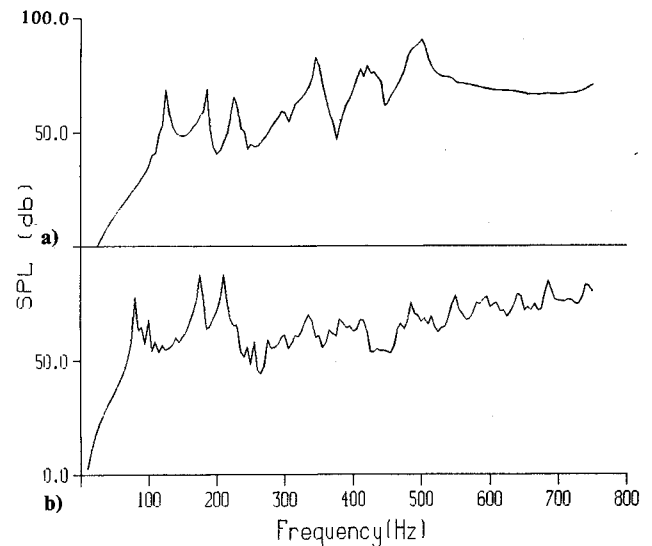


Fig. 3 Sound pressure levels at the center of the acoustic enclosure with a flexible wall of forty bays: a) one row and b) two rows.

occur at the same frequencies in both sets of results, and the general trend of large and small peaks is maintained, with a maximum SPL near 500 Hz. The infinite impedance case shows the acoustic peaks well, particularly at higher frequency, while normal acoustic impedance tends to damp out these peaks. Also, note that the normal impedance results have lower SPL values than the high-impedance results overall.

Next, an acoustic enclosure with a one- or two-row, forty-bay flexible wall and normal acoustic wall impedance at the $z = \text{const}$ walls was investigated. This enclosure's geometry was defined by $l = 400 \text{ in.}$, $h = 80 \text{ in.}$, $d = 48 \text{ in.}$, $l_0 = 36 \text{ in.}$, and $L_x = 328 \text{ in.}$; also, the one-row case had $h_0 = 30 \text{ in.}$ and $L_y = 20 \text{ in.}$, while the two-row case had $h_0 = 20 \text{ in.}$ and $L_y = 40 \text{ in.}$ Again, the SPL is evaluated at the geometric center of the enclosure. The single-row results are found in Fig. 3a, while the double-row results are found in Fig. 3b. The frequencies of the primary structural-acoustic peaks correlate well between the two cases, with the exception of the first peak. This first peak frequency differs significantly between cases because the first structural mode occurs at a lower frequency for the two-row wall than for the one-row wall, and this is borne out in the results. Also, there are more small peaks evident in the two-row case, because the two-row wall's structural response is more complex, especially at higher frequencies.

An actual fuselage section will have a skin-stringer-frame structure with many rows and bays, and noise transmission into a typical fuselage will be complicated. Nevertheless, noise transmission into simple acoustic enclosures will be similar to noise transmission into full fuselages. The SPL results in this work contain a few dominant acoustic-structural peaks, with smaller perturbations which are more noticeable in enclosures with more rows in the flexible wall, and in smaller enclosures with fewer bays. Results for a full fuselage should bear more resemblance to the two-row forty-bay results in Fig. 3b than to any of the one-row results; the authors confirmed this by analyzing the forty-bay acoustic enclosure with a three-row forty-bay flexible wall, and found that the noise transmission for this case bore a strong resemblance to that of the two-row case.

The finite element-decaying wave method (FEDW) was used to do all structural response analysis for this work. The FEDW method has the ease of formulation of a finite element method, the low memory requirements of a transfer-matrix technique, and the numerical stability of a wave-propagation approach, making it a good numerical method to use for the structural problem. The finite element method would also be a good method to use for this analysis, and would in fact be faster than the FEDW approach, but would use more memory and give less-accurate results for the same discretization.

Acknowledgment

This work was supported by NSF Grant MSM-9008953.

References

- ¹Vaicaitis, R., and Slazak, M., "Noise Transmission Through Stiffened Panels," *Journal of Sound and Vibration*, Vol. 70, No. 3, 1980, pp. 413-426.
- ²Lyrantzis, C. S., and Vaicaitis, R., "Structure-Borne Noise Generation and Transmission," *Journal of Probabilistic Engineering Mechanics*, Vol. 2, No. 3, 1987, pp. 114-120.
- ³Lyrantzis, C. S., and Bofilios, D. A., "Hygrothermal Effects on Structure-Borne Noise Transmission of Stiffened Laminated Composite Plates," *Journal of Aircraft*, Vol. 27, No. 8, 1990, pp. 722-730.
- ⁴Bofilios, D. A., and Lyrantzis, C. S., "Structure-Borne Noise Transmission into Cylindrical Enclosures of Finite Extent," *AIAA Journal*, Vol. 29, No. 8, 1991, pp. 1193-1201.
- ⁵Huntington, D. E., and Lyrantzis, C. S., "Dynamics of Skin-Stinger Panels Using Modified Wave Methods," *AIAA Journal*, Vol. 30, No. 11, 1992, pp. 2765-2773.
- ⁶McDaniel, T. J., and Eversole, K. B., "A Combined Finite Element-Transfer Matrix Structural Analysis Method," *Journal of Sound and Vibration*, Vol. 51, No. 2, 1977, pp. 157-169.
- ⁷Yong, Y., and Lin, Y. K., "Propagation of Decaying Waves in Periodic and Piece-Wise Periodic Structures," *Journal of Sound and Vibration*, Vol. 129, No. 1, 1989, pp. 99-118.

Supersonic Jet Control via Point Disturbances Inside the Nozzle

D. P. Wishart* and A. Krothapalli†

Florida A&M University and Florida State University,
Tallahassee, Florida 32316

and

M. G. Mungal‡

Stanford University, Stanford, California 94305

Introduction

IT is well known that the directivity of sound generated by a supersonic jet depends largely on the shape of the jet column and its development. For example, considerable side-line noise reduction was achieved on a Concorde nozzle by squeezing of the axisymmetric jet in the horizontal plane.^{1,2} This observation resulted in studies of notched nozzles obtained by cutting wedge shaped notches in the originally conical nozzle.^{2,3} The resultant flowfield from the notched nozzle was found to consist of large streamwise vortices shed from the swept edges of the notches² and is primarily responsible for the distortion of the jet. Similar distortion of an axisymmetric jet was also observed by placing tabs at the exit of the nozzle.⁴⁻⁶ In this work, we discuss a novel means by which supersonic jets can be significantly perturbed using single point disturbances that generate streamwise vortices. The present work is the round jet equivalent of the Side-Wall Shock Vortex Generator (SWSVG) recently described by Clemens and Mungal⁷ for two-dimensional supersonic mixing layers. In their work it was suggested that shock wave disturbances launched from the wall inside a supersonic nozzle could interact with the splitter tip producing streamwise vortices that lead to significant roll-up of the layer. In this work, we continue this approach of launching disturbances from within a supersonic nozzle in order to generate streamwise vortices that distort the jet column.

Received Nov. 27, 1992; revision received Dec. 21, 1992; accepted for publication Dec. 22, 1992. Copyright © 1993 by the American Institute of Aeronautics and Astronautics, Inc. All rights reserved.

*Graduate Student, Department of Mechanical Engineering. Member AIAA.

†Professor and Chairman, Department of Mechanical Engineering. Member AIAA.

‡Associate Professor, Department of Mechanical Engineering. Member AIAA.

Experimental Details

The experiments described here were performed at the Fluid Mechanics Research Laboratory of Florida A&M University and Florida State University, using a pressure matched converging-diverging nozzle with an exit diameter of 3.11 cm and exit Mach number of 2.1. The stagnation temperature was nominally room temperature. Figure 1 shows a sketch of the nozzle together with the technique used for providing point disturbances within the supersonic nozzle region; small rods (diam=1.6 mm, penetration depth=4.8 mm) were inserted externally to the nozzle using a set screw mechanism at several locations between the throat and exit plane. Machining constraints dictated that the disturbance rods projected upstream at an angle of 28 deg to the jet centerline. Each point disturbance emits a cone shaped disturbance wave; the intersection of the cone and the nozzle lip produces two regions of pressure mismatch that cannot be sustained by the shear layer, and a pair of streamwise vortices are formed.⁷

Four cases were investigated as shown in Fig. 2. If the nozzle exit were viewed from downstream, looking upstream, with 12 o'clock corresponding to the top edge of the nozzle, the cases were 1) undisturbed nozzle; 2) single disturbance at $x=-2.54$ cm, 3 o'clock position; 3) two disturbances at $x=-2.54$ cm, 3 and 9 o'clock positions; and 4) two disturbances, $x=-1.59$ cm at 12 o'clock and $x=-2.54$ cm at 3 o'clock. The local Mach numbers at the disturbance locations $x=-2.54$ and -1.59 cm are 1.9 and 2.0, respectively. Condensation of moisture from the ambient room air that mixes with the cold jet fluid produces a fine condensate fog that marks the mixing region, hence the flow is visualized using the planar laser Mie scattering technique⁸ with light pulses (10 ns pulse duration) from a frequency doubled Nd:Yag laser (532 nm, 100 mJ per pulse).

Results and Discussion

Figures 3a-d show views of the jet mixing layer (looking upstream) at a station 3.75 diam downstream of the jet exit. Three images are shown for each case, two instantaneous realizations and a multiple exposure consisting of 20 to 30 independent realizations used to define an ensemble average. The viewing angle of the camera was approximately 30 deg to the jet centerline, and so some distortion is observable.

Figure 3a shows results for the undisturbed nozzle and is used as a basis for comparison. Distortion of the jet mixing layer is comparable to similar views of ideally expanded supersonic jets seen earlier.⁹ The ensemble average shows the expected doughnut shape of the jet mixing layer. Figure 3b shows results for a single disturbance, case 2. Here considerable distortion is observed and results from the shock wave disturbance interacting with the lip of the jet (see Fig. 1) inducing roll-up of the jet shear layer. The disturbance is observed throughout the jet, resulting in a polygonal appearance, even though the disturbance generator is applied at the 3 o'clock position. The effect, however, is somewhat more pronounced at the 3 o'clock position. Figure 3c shows that two symmetrically placed disturbances, case 3, convert the jet to a more rectangular and (vertically) symmetric appearance with prominent corner cusps; a similar appearance was also observed further downstream. Figure 3d shows that two asymmetric disturbances produce a more complex, star-like appearance. Because both dis-

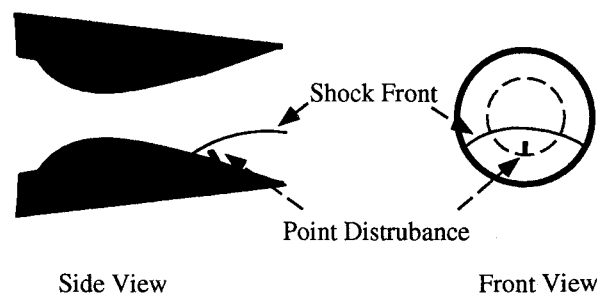


Fig. 1 Sketch of supersonic nozzle, disturbance generator, and internal disturbance wave.